

# Effect of Turbulent Model on the Accuracy of Numerical Simulation of Incompressible Flow over Backward Facing Step

S.R Sabbagh-Yazdi<sup>1</sup>, M Bavandpour<sup>2,\*</sup>

*1, Professor, Civil Engineering Department, KN Toosi University of Technology, Tehran-19697, Iran*

*2, MSc Student, Civil Engineering Department, KN Toosi University of Technology, Tehran-19697, Iran*

---

## ARTICLE INFO

### Article history:

**Received:** 4 March 2023

**Accepted:** 2 April 2023

### Keywords:

*Turbulent Model*

*Recirculation Zone*

*Backward-Facing Step*

---

## ABSTRACT

This study investigates effect of turbulence models and boundary layer simulation methods on the accuracy and run time of numerical simulation of the recirculation zone after the backward facing step. Expansion ratio and aspect ratio of the backward-facing step are 2.02 and 8, respectively. The numerical simulations are conducted in 6847 and 4926 Reynolds number (based on the hydraulic diameter of inlet channel and average inlet velocity). The Shear Stress Transport (SST) and the standard turbulence models are utilized and two cases of unstructured mesh are considered: 1) near-wall coarse mesh and 2) near-wall fine mesh. The results show that the SST turbulence model predicts the reattachment length more accurately than the model along with enhanced wall treatment. Although, the standard model is less accurate, its required CPU time is significantly shorter than the SST model. This study investigates effect of turbulence models and boundary layer simulation methods on the accuracy and run time of numerical simulation of the recirculation zone after the backward facing step. Expansion ratio and aspect ratio of the backward-facing step are 2.02 and 8, respectively. The numerical simulations are conducted in 6847 and 4926 Reynolds number (based on the hydraulic diameter of inlet channel and average inlet velocity). The Shear Stress Transport (SST) and the standard turbulence models are utilized and two cases of unstructured mesh are considered: 1) near-wall coarse mesh and 2) near-wall fine mesh. The results show that the SST turbulence model predicts the reattachment length more accurately than the model along with enhanced wall treatment. Although, the standard model is less accurate, its required CPU time is significantly shorter than the SST model..

---

\*Corresponding author's email: [majid.bavandpour@gmail.com](mailto:majid.bavandpour@gmail.com)

## 1. Introduction

Accuracy of numerical simulation results can be affected by various factors such as computational domain, mesh distribution, boundary layer modelling methods, turbulence models and etc. Backward-facing step is a fundamental flow in fluid mechanic and reattachment length after step can be used for assessment of the methods applied in computational fluid dynamic (CFD). For this purpose, numerical simulation results ought to be compared with the experimental results.

Many researchers have conducted the numerical simulations on the reattachment length of the flow after backward-facing step. [1] And [2] are the experimental works performed in a wide range of flow regimes (laminar, transient and turbulent), and have been used to verify the numerical simulation results of two-dimensional and three-dimensional backward-facing step, respectively. [3], [4] and [5] used the numerical simulation to study the flow over backward-facing step which had been experimentally modelled by [1]. And also, [6] simulated numerically the backward-facing step which had been experimentally modelled by [2]. Here, the simulation results of three-dimensional backward-facing step models are compared with the results of Ref. [2].

This study investigates the effect of turbulence models and boundary layer modelling methods on the reattachment length that takes place after backward-facing step. The governing equations and turbulence models are presented in section 2. Then, characteristics of computational domain, such as the geometry of the domain and boundary conditions, and also numerical methods for solving equations are described in the section 3. Finally, results and conclusion of paper is presented in section 4.

## 2. Materials and Methods

For accurate prediction of a given physical phenomenon, its governing equations ought to be known. In the first subsection, the governing equations of fluid flow are presented. Turbulence models applied in this paper are then briefly described in the second subsection.

### 2.1. Navier-Stokes equations

Governing equations of incompressible turbulent fluid flow over the three-dimensional backward-facing step can be expressed as:

$$\text{div}(\mathbf{V}) = 0 \quad (1)$$

$$\frac{\partial u}{\partial t} + \text{div}(u \mathbf{V}) = \frac{1}{\rho} \left( \frac{-\partial P}{\partial x} + \text{div}(\mu \text{ grad } u) \right) \quad (2)$$

$$\frac{\partial v}{\partial t} + \text{div}(v \mathbf{V}) = \frac{1}{\rho} \left( \frac{-\partial P}{\partial y} + \text{div}(\mu \text{ grad } v) \right) \quad (3)$$

$$\frac{\partial w}{\partial t} + \text{div}(w \mathbf{V}) = \frac{1}{\rho} \left( \frac{-\partial P}{\partial z} + \text{div}(\mu \text{ grad } w) \right) \quad (4)$$

where,  $\rho$  is the mass density of fluid,  $t$  is the time,  $\mathbf{V}$  is the velocity vector,  $P$  is the static pressure,  $\mu$  is the dynamic viscosity,  $u$ ,  $v$  and  $w$  are respectively the velocity vector components in the  $x$ ,  $y$  and  $z$  directions [7].

### 2.2. Turbulence models

In this study, standard  $k-\varepsilon$  model along with enhanced wall treatment and SST  $k-\omega$  turbulence model is employed. The standard  $k-\varepsilon$  turbulence model is a two-equation turbulence model. Partial differential equations for the turbulent kinetic energy ( $k$ ) and the turbulent dissipation rate ( $\varepsilon$ ) in the standard  $k-\varepsilon$  model can be expressed as [8]:

$$\frac{\partial k}{\partial t} + \frac{\partial(ku_i)}{\partial x_i} = \frac{1}{\rho} \frac{\partial}{\partial x_j} \left[ \left( \mu + \frac{\mu_t}{\sigma_k} \right) \frac{\partial k}{\partial x_j} \right] + \nu_t S^2 - \varepsilon + S_k \quad (5)$$

$$\frac{\partial \varepsilon}{\partial t} + \frac{\partial(\varepsilon u_i)}{\partial x_i} = \frac{1}{\rho} \frac{\partial}{\partial x_j} \left[ \left( \mu + \frac{\mu_t}{\sigma_\varepsilon} \right) \frac{\partial \varepsilon}{\partial x_j} \right] + C_{1\varepsilon} \frac{\varepsilon}{k} (\nu_t S^2) - C_{2\varepsilon} \frac{\varepsilon^2}{k} + S_\varepsilon \quad (6)$$

where,  $\mu_t$  is the turbulent viscosity,  $S_k$  and  $S_\varepsilon$  are source terms,  $\sigma_k$  and  $\sigma_\varepsilon$  are the turbulent Prandtl number for  $k$  and  $\varepsilon$  respectively,  $C_{1\varepsilon}$  and  $C_{2\varepsilon}$  are constants and  $S$  is the modulus of mean rate-of-strain tensor which can be calculated using the following formula:

$$S \equiv \sqrt{2S_{ij}S_{ij}} \quad , \quad S_{ij} = \frac{\partial u_i}{\partial x_j} + \frac{\partial u_j}{\partial x_i} \quad (7)$$

The turbulent viscosity ( $\mu_t$ ) is computed by:

$$\mu_t = \rho C_\mu \frac{k^2}{\varepsilon} \quad (8)$$

where,  $C_\mu$  is a constant parameter. Closure coefficients for above equations are:

$$\sigma_k = 1.0, \sigma_\varepsilon = 1.3, C_{1\varepsilon} = 1.44, C_{2\varepsilon} = 1.92, C_\mu = 0.09$$

The SST  $k-\omega$  turbulence model is a  $k-\omega$  based model. Therefore, in this model, two partial differential transport equation is solved for the turbulent kinetic energy ( $k$ ) and specific turbulent dissipation rate ( $\omega$ ). The SST  $k-\omega$  turbulence model uses the standard  $k-\omega$  model for modelling near-wall regions, and the standard  $k-\varepsilon$  model for modelling the regions far from the walls. The partial differential equations for this model are [9]:

$$\frac{\partial k}{\partial t} + \frac{\partial(ku_i)}{\partial x_i} = \frac{1}{\rho} \frac{\partial}{\partial x_j} \left[ \left( \mu + \frac{\mu_t}{\sigma_k} \right) \frac{\partial k}{\partial x_j} \right] + \tilde{G}_k - \beta^* k \omega + S_k \quad (9)$$

$$\frac{\partial \omega}{\partial t} + \frac{\partial(\omega u_i)}{\partial x_i} = \frac{1}{\rho} \frac{\partial}{\partial x_j} \left[ \left( \mu + \frac{\mu_t}{\sigma_\omega} \right) \frac{\partial \omega}{\partial x_j} \right] + \alpha S^2 - \beta_1 \omega^2 + D_\omega + S_\omega \quad (10)$$

Auxiliary relations for above equations are:

$$\sigma_k = \frac{1}{(F_1/1.176) + (1-F_1)}$$

$$\sigma_\omega = \frac{1}{(F_1/2) + [(1-F_1)/1.168]}$$

$$\tilde{G}_k = \min(v_t S^2, 10\beta^* k \omega)$$

$$\beta^* = 0.09 \left( \frac{4/15 + (\text{Re}_t/8)^4}{1 + (\text{Re}_t/8)^4} \right), \quad \alpha = \frac{\alpha_\infty}{\alpha^*} \left( \frac{\alpha_0 + \text{Re}_t/2.95}{1 + \text{Re}_t/2.95} \right)$$

$$\alpha^* = \frac{\beta_i/3 + \text{Re}_t/6}{1 + \text{Re}_t/6}, \quad \text{Re}_t = \frac{\rho k}{\mu \omega}$$

$$\alpha_\infty = 0.553F_1 + 0.44(1-F_1), \quad \beta_i = 0.075F_1 + 0.0828(1-F_1)$$

$$D_\omega = 2(1-F_1)\sigma_{\omega,2} \frac{1}{\omega} \frac{\partial k}{\partial x_j} \frac{\partial \omega}{\partial x_j}$$

where,  $\tilde{G}_k$  is the generation of turbulence kinetic energy due to mean velocity gradient,  $S_k$  and  $S_\omega$  are source terms. The switching function is defined as [10]:

$$F_1 = \tanh(\arg_1^4), \quad F_2 = \tanh(\arg_2^2) \quad (11)$$

$$\arg_1 = \min \left[ \max \left( \frac{\sqrt{k}}{0.09\omega d}, \frac{500\mu}{\rho d^2 \omega} \right), \frac{4\rho k}{\sigma_{\omega,2} CD_{k,\omega} d^2} \right] \quad (12)$$

$$CD_{k,\omega} = \max \left( 2\rho \frac{1}{\sigma_{\omega,2}} \frac{1}{\omega} \frac{\partial k}{\partial x_j} \frac{\partial \omega}{\partial x_j}, 10^{-10} \right) \quad (13)$$

$$\arg_2 = \max \left( 2 \frac{\sqrt{k}}{0.09\omega d}, \frac{500\mu}{\rho d^2 \omega} \right) \quad (14)$$

where,  $F_1$  and  $F_2$  are the blending functions,  $d$  is the distance to the nearest wall and  $\sigma_{\omega,2}$  is a constant parameter which is equal to 1.168. The turbulent viscosity ( $\mu_t$ ) is computed by:

$$\mu_t = \frac{\rho k}{\omega} \frac{1}{\max \left[ \frac{1}{\alpha^*}, \frac{SF_2}{a_1 \omega} \right]} \quad (15)$$

where,  $S$  is the strain rate magnitude and  $a_1$  is a constant parameter which is equal to 0.31.

### 2.3. Computational Domain

In this study, the reattachment length after the step is selected for assessing the turbulence models. The backward-facing step with expansion ratio 2.02 and aspect ratio 8 is considered. The numerical simulations are conducted in the 6847 and 4926 Reynolds number (based on the hydraulic diameter of inlet channel and average inlet velocity) and results of the numerical simulation are compared with available experimental data [2]. Fig. 1 shows a schematic view of the computational domain and boundary conditions of the backward-facing step. The step height ( $S$ ) is 1 cm, channel height before the

step (h) and channel height after the step (H) are 0.98 cm and 1.98 cm, respectively. The channel width (w) is 8 cm but due to the symmetry condition of the flow in the channel, half of the channel is considered and symmetry plane boundary condition is used instead. Because of using the fully developed velocity profile fitted to the experimental data [2] for inlet boundary condition, Length of the inlet channel is considered equal to the step height. Length of the channel after the step (L) is 40cm (40S). This length ensures that the flow downstream of the step be fully developed again.

No-slip boundary condition ( $u = 0, v = 0, w=0$ ) is employed for all the walls and symmetry boundary condition is employed for the right side of the domain and half of the domain is not considered. The fully developed velocity profile fitted to the experimental data is applied to the inlet plane. For the outlet plane, flux diffusion of all flow variables in the outlet direction are set to zero.

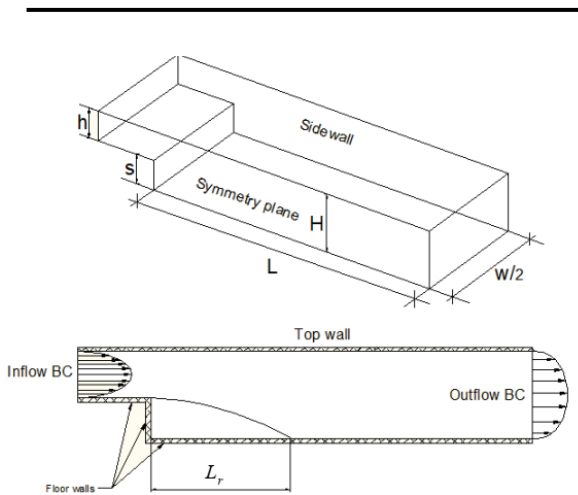
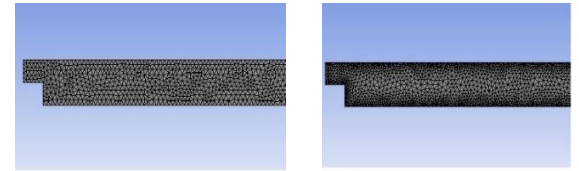


**Fig.1.** Schematic view of the computational domain geometry and boundary conditions

The above partial differential equations are solved with ANSYS FLUENT software and the finite volume method (FVM) is employed for discretizing these equations. For obtaining the pressure field and linking pressure field and velocity field, the Semi-Implicit Method for Pressure-Linked Equations (SIMPLE) algorithm is used. These equations are solved on the tetrahedral element. Fig. 2 (a) shows the unstructured near-wall fine mesh for the SST  $k-\omega$  turbulence model without wall function ( $y^+ \approx 1$ ) and Fig. 2 (b) shows the unstructured near-wall coarse

mesh for the  $k-\varepsilon$  turbulence model with enhanced wall treatment.



**a)** Without wall-function      **b)** With wall-function

**Fig.2.** Unstructured mesh of the backward-facing step

### 3. Results and discussions

Due to separation of the flow on the step, primary recirculation zone after the step takes place. Fig. 3 shows the primary recirculation zone after the step in the 6847 Reynolds number that obtained by SST  $k-\omega$  turbulence model and without wall function. Even though this study focuses on the reattachment length of the primary recirculation zone, secondary recirculation zone on the top wall is captured (see Fig. 3).

The reattachment length is defined as the distance between the edge of step to the point with zero velocity in flow direction ( $u=0$ ). The results of numerical simulation such as simulation CPU time and the reattachment length of every simulation case are given in table 1. In this table, the error of estimations ( $Er$ ) is calculated by:

$$Er = \frac{L_{r,exp} - L_{r,num}}{L_{r,exp}} \times 100 \quad (16)$$

where,  $L_{r,exp}$  is the experimental reattachment length and  $L_{r,num}$  is the numerical simulation reattachment length.

The results show that the SST  $k-\omega$  turbulence model in comparison with the  $k-\varepsilon$  model has more plausible results considering experimental data, but needs more CPU time. Because of using the enhanced wall function in the  $k-\varepsilon$  model, required number of

elements is reduced and consequently the total CPU time and accuracy of the results are reduced.

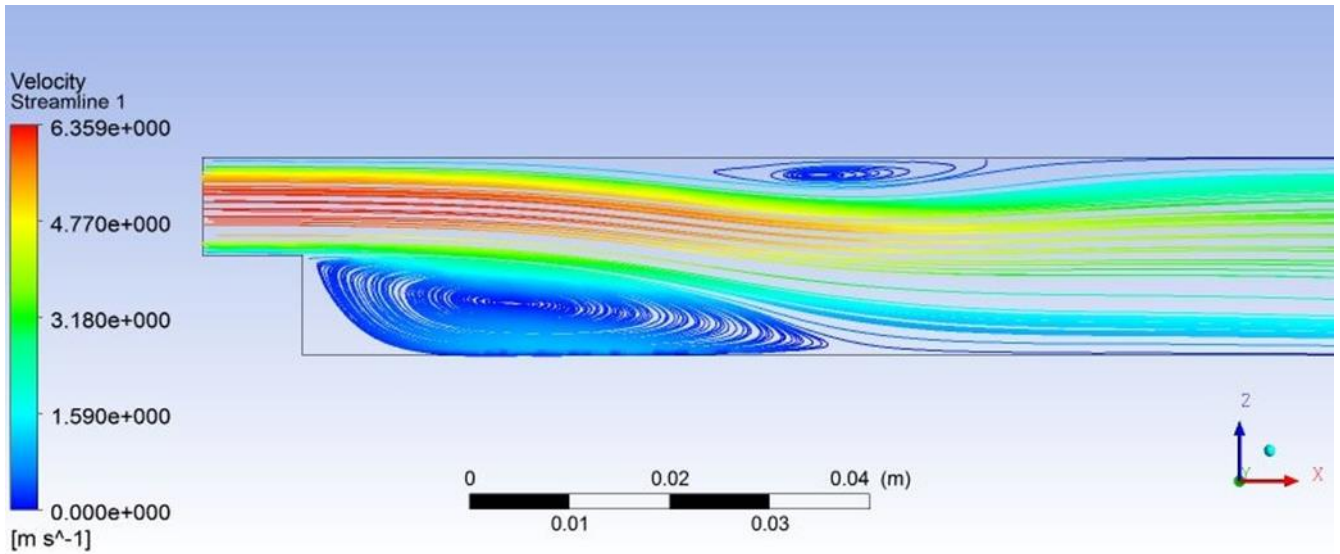


Fig.3 Streamline of velocity in Re=6847

Table 1. Results of numerical simulations

Re	Simulation results( $L_r/S$ )		Exp ( $L_r/S$ )	Error (%)		Total CPU Time(s)	
	SST k- $\omega$	k- $\epsilon$		SST k- $\omega$	k- $\epsilon$	SST k- $\omega$	k- $\epsilon$
6847	6.6	4.27	6.65	0.752	35.79	126734	9662
4926	6.19	4.20	6.33	2.212	33.65	125801	10302

#### 4. Conclusion

For simulation of the flow over the three-dimensional backward facing step the standard  $k-\epsilon$  model along with enhanced wall treatment and the SST  $k-\omega$  turbulence model is used. Assessment of the accuracy and run time of these models show that the SST  $k-\omega$  model along with refinement mesh near the walls is an accurate model and can be used where the minimum required accuracy is relatively high. Also, the  $k-\epsilon$  model is an economic model which is used for initial estimating in engineering applications with less computational cost.

#### 5.References

1. Armaly, B., Durst, F., Pereira, J., & Schonung, B. (1983). Experimental and theoretical investigation of backward-facing step flow. *Journal of Fluid Mechanics*, 127, 473–496.
2. Nie, J. H., & Armaly, B. F. (2004). Reverse flow regions in three-dimensional backward-facing step flow. *International Journal of Heat and Mass Transfer*, 47 (22), 4713–4720.
3. Le, H., Moin, P., & Kim, J. (1997). Direct numerical simulation of turbulent flow over a backward-facing step. *Journal of Fluid Mechanics*, 330, 349–374.
4. Biswas, G., Breuer, M., & Durst, F. (2004). Backward-Facing Step Flows for Various Expansion Ratios at Low

and Moderate Reynolds Numbers. *Journal of Fluids Engineering*, 126(3), 362.

**5.** Ratha, D., & Sarkar, A. (2014). Analysis of flow over backward facing step with transition. *Frontiers of Structural and Civil Engineering*, 9(1), 71–81.

**6.** Rani, H. P., Sheu, T. W. H., & Tsai, E. S. F. (2007). Eddy structures in a transitional backward-facing step flow. *Journal of Fluid Mechanics*, 588, 43–58.

**7.** Versteeg, H.K. and Malalaskera, W., (1995), “An introduction to Computational Fluid Dynamics, The Finite Volume Method,” Harlow, UK: Longman.

**8.** Wilcox, D. C. (1998). *Turbulence modeling for CFD* (ol. 2, pp. 103-217). La Canada, CA: DCW industries.

**9.** Menter, F. R. (1994). Two-equation eddy-viscosity turbulence models for engineering applications. *AIAA journal*, 32(8), 1598-1605.

**10.** Haque, A., Ahmad, F., Yamada, S., & Chaudhry, S. R. (2007). Assessment of Turbulence Models for Turbulent Flow over Backward Facing Step. In *Proceedings of the World Congress on Engineering* (Vol. II, pp. 2–7).